

The Silkmoth Eggshell as a Natural Amyloid Shield for the Safe Development of Insect Oocyte and Embryo: Insights From Studies of Silkmoth Chorion Protein Peptide-Analogues of the B Family

Vassiliki A. Iconomidou,¹ Paul Cordopatis,² Andreas Hoenger,³ Stavros J. Hamodrakas¹

¹Department of Cell Biology and Biophysics, Faculty of Biology, University of Athens, Panepistimiopolis, Athens 157 01, Greece

²Department of Pharmacy, Laboratory of Pharmacology and Chemistry of Natural Products, University of Patras, 26500 Patras, Greece

³Department of Molecular Cellular and Developmental Biology, University of Colorado at Boulder, Boulder CO, 80309-0347

Received 30 July 2010; revised 15 November 2010; accepted 1 February 2011

Published online 18 February 2011 in Wiley Online Library (wileyonlinelibrary.com). DOI 10.1002/bip.21606

ABSTRACT:

Silkmoth chorion is the major component of the silkmoth eggshell. The proteins that constitute more than 95% of its dry mass have remarkable mechanical and physicochemical properties forming a protective natural shield for the oocyte and the developing embryo from a wide range of environmental hazards. Peptide-analogues of the central conservative domain of the two major families of silkmoth chorion proteins, the A's and the B's, form amyloid fibrils under a variety of conditions, which prompted us to propose, 10 years ago, that silkmoth chorion is an amyloid with protective properties. Following our finding, a number of studies verified the existence of several functional amyloids. In this study, we designed, synthesized and studied two peptide-analogues of the central conservative domain of the B family of silkmoth chorion proteins, and we present experimental results, which show: (a) that the amyloidogenic properties of silkmoth chorion peptides are encoded into the tandemly repeating hexapeptides comprising the central

domain of silkmoth chorion proteins, confirming our previous findings from peptide analogues of the A family of chorion proteins, and, (b) they suggest how silkmoth chorion proteins of the B family self-assemble *in vivo*, for the formation of the helicoidal architecture of silkmoth chorion. © 2011 Wiley Periodicals, Inc. *Biopolymers* (Pept Sci) 96: 723–733, 2011.

Keywords: silkmoth chorion proteins; amyloid fibrils; electron microscopy; X-ray diffraction; ATR FT-IR spectroscopy; B family silkmoth chorion protein peptide-analogues; modeling

This article was originally published online as an accepted preprint. The "Published Online" date corresponds to the preprint version. You can request a copy of the preprint by emailing the *Biopolymers* editorial office at biopolymers@wiley.com

INTRODUCTION

Silkmoth chorion is a proteinaceous layer, which is the major component (90%) of the insect's eggshell. It has extraordinary mechanical and physicochemical properties, protecting the oocyte and the developing embryo from diverse environmental hazards such as mechanical pressures, temperature variations, desiccation, proteases, bacteria, viruses, etc, and also provides for important physiological functions, allowing sperm entry-fertilization, exchange of respiratory gases etc.¹ About 200 proteins have been detected in silkmoth chorion,² which have been classified into two major classes, or families, the A and B¹.

Correspondence to: Stavros J. Hamodrakas; e-mail: shamodr@biol.uoa.gr

Contract grant sponsor: University of Athens

© 2011 Wiley Periodicals, Inc.

as, B_m1, is six residues longer than the consensus 18-residue B-peptide (see Figure 1), differing from the 18-residue B peptide⁷ at a single amino acid position (an asparagine, N has been replaced by a glutamate, E, see Figure 1). This is a variation commonly found in silkmoth chorion proteins of the B family, with asparagine more frequent than glutamate at this position.⁵ The extra six residues were taken from the consensus sequence representing the entire central domain of the B family of silkmoth chorion proteins.⁵ The second peptide, called B_m2, is a variant of the first, having two hydrophobic residues (a valine, V, and a leucine, L) replaced by glutamates (E) at specific positions (see Figure 1). We designed these peptides because we wanted to find out: (a) whether an increase of the length of the B peptide by the basic repeat of six residues would still produce amyloid-like fibrils and, (b) whether the unique sequences of chorion proteins selected after millions of years of molecular evolution for the formation of chorion fibrils, may withstand suitably selected mutations, which may affect formation of amyloid-like fibrils. We should perhaps mention at this point that, B_m1 has a length ca. one half (1/2) of the consensus of the central domain of the B family of proteins (that is, it accounts for ca. 10–15% of the total chorion proteinaceous mass). Furthermore, by performing these experiments, we aimed at a deeper understanding of the specific roles of chorion proteins in the architectural design of the helicoidal structure of silkmoth chorion.

In this work, we report on the self-assembly properties of these two new B family peptide-analogues, and discuss the implications of our findings in relation to the structure of silkmoth chorion.

MATERIALS AND METHODS

Formation of Amyloid-Like Fibrils

B_m1 and B_m2 peptides (see Figure 1), synthesized in a similar way as described previously,¹³ were dissolved: (a) in distilled water (pH 5.5), (b) in a 50 mM sodium acetate buffer (pH 5) and (c) in a 50% (w/v) water/methanol mixture, at a concentration of 10 mg ml⁻¹. B_m1 peptide formed, in all cases, mature amyloid-like fibrils after one to two weeks incubation, in contrast to the solutions of the B_m2 peptide, which did not produce amyloid-like fibrils even after incubation for several months. The fibrils formed from B_m1 peptide solutions were judged to be mature, examining them both for shorter and longer incubation times than one to two weeks.

X-Ray Diffraction

B_m1 peptide was dissolved in a 50% (w/v) water/methanol mixture, at a concentration of 10 mg ml⁻¹ to produce mature amyloid-like fibrils after one to two weeks incubation. A droplet (~10 μl) of

fibril suspension was placed between two siliconized glass rods, spaced ~2 mm apart and mounted horizontally on a glass substrate, as collinearly as possible. The droplet was allowed to dry slowly at ambient temperature and humidity for 1 h to form an oriented fiber suitable for X-ray diffraction. X-ray diffraction patterns were recorded on a Mar Research 345 mm image plate, utilizing double-mirror (Prophysics mirror system XRM-216) focused CuK_α radiation ($\lambda = 1.5418 \text{ \AA}$), obtained from a GX-21 rotating anode generator (Elliot-Marconi Avionics, Hertfordshire, England) operated at 40 kV, 75 mA. The specimen-to-film distance was set at 150 mm and the exposure time was 30 min. No additional low angle reflections were observed at longer specimen-to-film distances of up to 300 mm. The X-ray patterns, initially viewed using the program MarView (MAR Research, Hamburg, Germany), were displayed and measured with the aid of the program IPDISP of the CCP4 package.¹⁴

Negative Staining

For negative staining, the B_m1 peptide fibril suspensions as well as the B_m2 solutions after incubation for several months, were applied to glow-discharged 400-mesh carbon coated copper grids for 60 s. The grids were, occasionally, flash-washed with ca. 150 μl of distilled water and stained with a drop of 1% (w/v) aqueous uranyl acetate for 45 s. Excess stain was removed by blotting with a filter paper and the grids were air-dried. They were examined in a Philips CM120 Biotwin transmission electron microscope operated at 100 kV or in a Philips Morgagni 268D electron microscope under the same conditions. EM micrographs were obtained by a retractable slow scan CCD camera (SSCTM, Gatan Inc.) utilizing the program Digital Micrograph 2.5.8 (Gatan Inc.).

Congo Red Staining and Polarized Light Microscopy

B_m1 peptide fibril suspensions were applied to glass slides and stained, while still in solution, with a 10 mM Congo red (Sigma) solution in phosphate-buffered saline (pH 7.4) for ~2 h, and then left to dry. They were then washed several times with 90% ethanol and left to dry. Subsequently, the samples were observed under bright field illumination and between crossed polars, using a Zeiss KL 1500 polarizing stereomicroscope equipped with an MC 80 DX camera.

Attenuated Total Reflectance Infrared Spectroscopy

Ten μl drops of the B_m1 or B_m2 suspensions, were cast separately on a front coated Au mirror and were left to dry slowly at ambient conditions to form thin films. Infrared spectra were obtained at a resolution of 4 cm⁻¹, utilizing an IR microscope (IRScope II by Bruker Optics), equipped with a Ge Attenuated Total Reflectance objective lens (20X) and attached to a Fourier-transform spectrometer (Equinox 55 by Bruker Optics). Internal reflection spectroscopy has several advantages compared to the more common KBr dispersion technique.¹⁵ The choice of ATR was dictated by the need to exclude any possible spectroscopic and chemical interactions between the sample and the dispersing medium. Having a penetration depth of less than 1 μm (1000 cm⁻¹, Ge), ATR is free of saturation effects, which may be present in the transmission spectra of thicker samples. Moreover, the use of the Ge ATR objective lens

facilitates the acquisition of data from small samples. Ten 32-scan spectra were collected from each sample and averaged to improve the S/N ratio.

The spectra are shown in the absorption mode after correction for the wavelength-dependence of the penetration depth ($d.p \propto \lambda$). Absorption peak maxima were determined from the minima in the 2nd derivative of the corresponding spectra computed by the Savitzky-Golay algorithm over a $\pm 8 \text{ cm}^{-1}$ range, around each data point.¹⁶

Smoothing over narrower ranges resulted to a deterioration of the S/N ratio and did not increase the number of minima that could be determined with confidence.

Modeling

Molecular homology modeling was performed following procedures described in detail earlier.⁶ The atomic models, the antiparallel β -pleated sheet and left-handed parallel β -helix, produced for the peptide cA in that work, were used as templates for the construction of the corresponding atomic models of the B_m1 and B_m2 peptides. The coordinates of the derived models are available on request. The software CLEARER¹⁷ was used to simulate X-ray diffraction fiber patterns from the models proposed for the B_m1 peptide. The parameters used to simulate the diffraction patterns were: For the antiparallel β -pleated sheet, a unit cell, with dimensions $a = 23.0 \text{ \AA}$ [chain axis direction along the antiparallel β -strands], $b = 9.4 \text{ \AA}$ [hydrogen bonding direction between β -strands (twice the distance between hydrogen bonded strands), fiber axis direction], $c = 10.2 \text{ \AA}$ [β -sheet stacking direction], $\alpha = \beta = \gamma = 90^\circ$ was chosen, and for the parallel left-handed β -helix, a unit cell with dimensions $a = 30.0 \text{ \AA}$ [packing distance between packed parallel left-handed β -helices], $b = 9.4 \text{ \AA}$ [hydrogen bonding direction between β -strands (twice the distance between hydrogen bonded strands)], $c = 23.0 \text{ \AA}$ [chain axis direction along the parallel β -strands], $\alpha = \beta = \gamma = 90^\circ$. In both cases, a crystallite size of 20 nm, 200 nm, 8 nm was used and this choice was dictated by the electron micrographs, and a fiber disorder of 0.3 radians.

RESULTS AND DISCUSSION

Contrasting Data From Analysis of the Two B Family Silkmoth Chorion Protein Peptide-Analogues

B_m1 peptide (see Figure 1) folds and self-assembles, forming mature amyloid-like fibrils (Figures 2a–2d) after one to two weeks incubation, in a variety of solvents and conditions (see Methods). In contrast, in solutions of B_m2, under the same conditions, after several months incubation, only very rarely, some ring-like fibril structures appear (see Figure 3). The fibrils formed by the B_m1 peptide are similar in structure and properties to the fibrils formed by the B peptide.⁷ They appear to be, most probably, double helical in structure (Figures 2a–2d), they bind Congo red showing the characteristic red-green birefringence when seen under crossed polars in a polarizing microscope (see Figure 4), and they give “cross- β ” X-ray diffraction patterns (see Figure 5) from ori-

ented fibers (see Methods) thus, displaying all the features that characterize amyloid fibrils. When cast as thin films on a front coated gold mirror and examined with ATR FT-IR spectroscopy, they produce IR spectra characteristic of antiparallel β -pleated sheet conformation (Figure 6a).

In detail: Suspensions of the B_m1 fibril-containing solutions seen in Figure 2, form oriented fibers (see Methods). X-ray diffraction patterns taken from these fibers (Figure 5) resemble “cross- β ” diffraction patterns obtained from amyloid fibrils.¹⁸ A strong meridional reflection at 4.65 \AA , representing the repetitive interchain distance between hydrogen bonded β -strands and a weak equatorial reflection at 10.2 \AA corresponding to the intersheet stacking periodicity, controlled by the amino acid side groups, which falls within the range 3.7 \AA ¹⁹ and 14.0 \AA .²⁰ This latter reflection is rather weak and diffuse presumably due to a short “crystallite” thickness in the so formed oriented fibers, as has been verified by the simulation of the X-ray diffraction patterns, utilizing the software CLEARER.¹⁷ There is a noticeable, also very strong, meridional reflection at 9.30 \AA ($4.65 \times 2 = \sim 9.3$), consistent with an antiparallel β -sheet structure.^{18–22} The origin of another, rather strong and sharp, meridional reflection at ca. 5.2 \AA , which, it should be noted, also appears in the X-ray diffraction patterns of the 18-residue B-peptide,⁷ is not clear (see also below).

Attempts to obtain oriented fibers from solutions of the B_m2 peptide (see Figure 1) were not successful since this peptide did not form amyloid like fibrils or suitable viscous solutions for fiber formation.

Spectral acquisition by ATR FT-IR spectroscopy has been shown to yield rich information about the secondary structure of the cA and also the B peptide, without the drawbacks associated with the more conventional vibrational techniques.^{7,23}

When B_m1 peptide suspensions containing amyloid fibrils were cast as thin films on a front coated gold mirror and examined with ATR FT-IR spectroscopy, they produced IR spectra, which provide concomitant evidence for the preponderance of antiparallel β -pleated sheet conformation (Figure 6a, Table I).

The ATR FT-IR spectrum of the B_m1 peptide amyloid-like fibrils shows one prominent band at 1626 cm^{-1} in the amide I region, an amide II band at 1520 cm^{-1} and an amide III weak band at 1229 cm^{-1} , which are all definitely due to β -sheet.^{24–27} The fact that the amide I band at 1626 cm^{-1} is sharp (its half-width is ca. 30 cm^{-1}) suggests that the distribution of the phi and psi angles in the sheets is rather narrow, which means a very uniform structure. Thus, ATR FT-IR supports the presence of uniform β -sheets in the structure of B_m1 peptide fibrils, in agreement with the existence of a

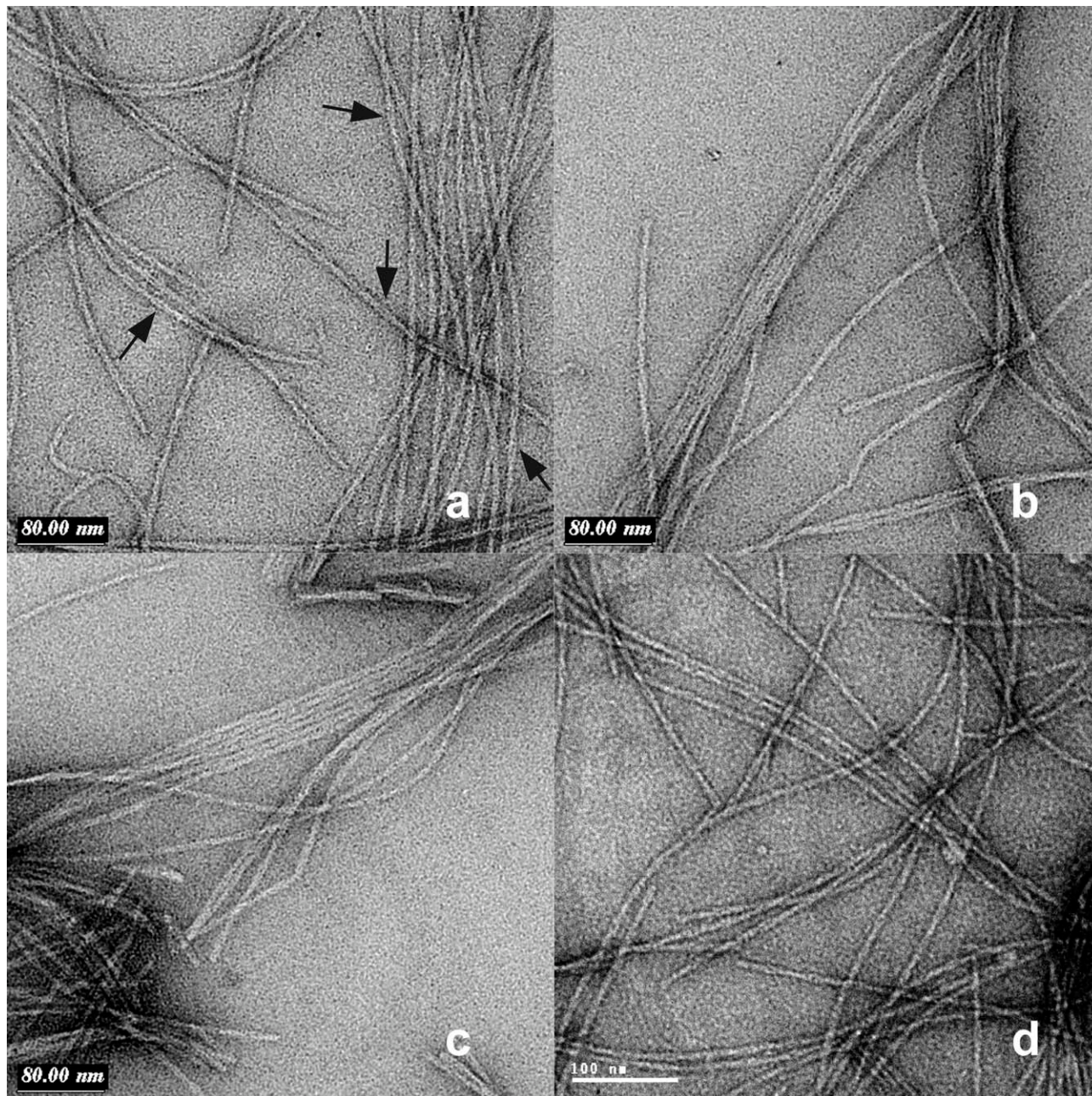


FIGURE 2 Electron micrographs of amyloid-like fibrils derived by self-assembly, from a 10 mg ml^{-1} solution of the B_{m1} peptide in distilled water, pH 5.5. Fibrils were negatively stained with 1% uranyl acetate. (a) They are of indeterminate length (several microns), unbranched, approximately $60\text{--}70 \text{ \AA}$ in diameter and have a double helical structure (arrows). A pair of protofilaments each $30\text{--}40 \text{ \AA}$ in diameter are frequently wound around each other, forming the double-helical fibrils. Bar 80 nm . (b, c) The fibrils have the tendency to coalesce laterally and in register among each other into twisted and nontwisted ribbons of short ($60\text{--}70 \text{ \AA}$) thickness and indeterminate length (several microns) forming gels (not shown). Bars 80 nm . (d) Fibrils produced by self-assembly, from a 50% (w/v) water/methanol mixture solutions of B_{m1} peptide, at a concentration of 10 mg ml^{-1} after negative staining, with 1% uranyl acetate, are also shown. Fibril characteristics as in (a) and (b) above. Bar 100 nm .

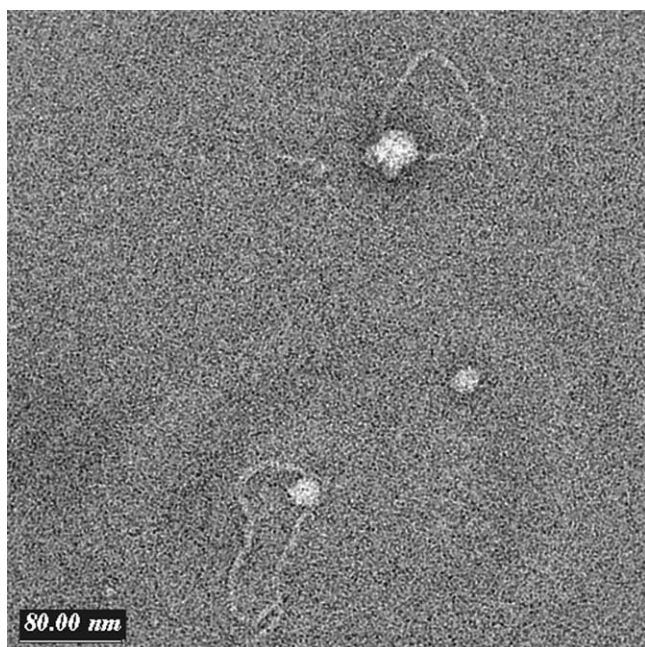


FIGURE 3 Electron micrograph of, very rarely appearing, ring-like structures derived by self-assembly, after incubation for several months, from a 10 mg ml^{-1} solution of the B_m2 peptide in a distilled water solution, pH 5.5. The grids were negatively stained with 1% uranyl acetate. Bar 80 nm.

β -sheet structure suggested by X-ray diffraction. The shoulder at 1690 cm^{-1} strongly suggests that the β -sheets are antiparallel, also in good agreement with X-ray data, and, another shoulder at 1659 cm^{-1} implies the presence of β -turns.^{24–27}

On the contrary, thin films cast from cA_m2 peptide solutions on front-coated gold mirrors produce ATR FT-IR spectra, characteristic of random coil structure of this peptide in these solutions (Figure 6b, Table I). The infrared band at

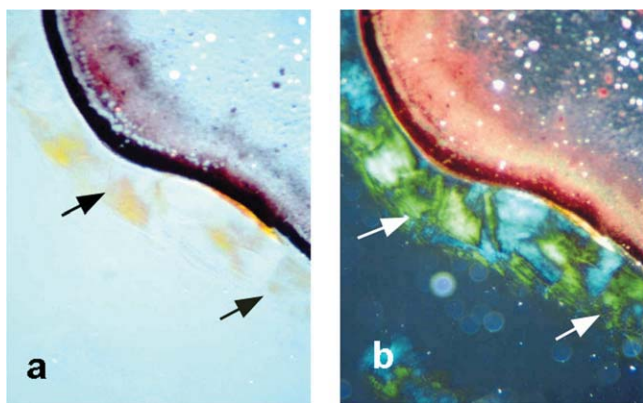


FIGURE 4 Photomicrographs of B_m1 peptide fibrils stained with Congo red: (a) Bright field illumination, (b) crossed polars. The red-green birefringence characteristic for amyloid fibrils is clearly seen (arrows).

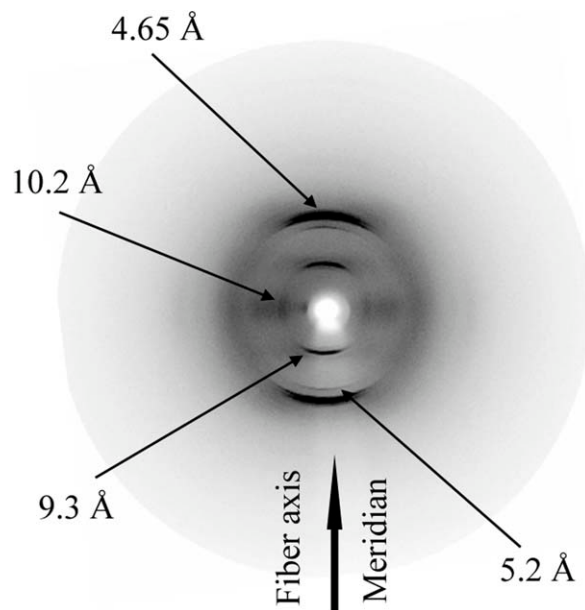


FIGURE 5 X-ray diffraction pattern from an oriented fiber of B_m1 peptide amyloid-like fibrils. The meridian, (direction parallel to the fiber axis) is vertical and the equator, is horizontal in this display. The X-ray diffraction pattern resembles a “cross- β ” pattern showing a strong meridional 4.65 \AA reflection and a weak 10.2 \AA reflection on the equator. The structural repeat of 4.65 \AA corresponds to the spacing of adjacent, hydrogen bonded, β -strands, perpendicular to the fiber axis and the 10.2 \AA spacing corresponds to the face-to-face separation (packing and stacking distance) of the β -sheets, parallel to the fiber axis. Possible origin and measured spacings of the other reflections are discussed into the text.

1645 cm^{-1} in the amide I region and the absence of any features in the amide III region are most probably indicative of random coil structure.^{24–27}

The ATR FT-IR spectra from B_m1 and B_m2 peptides (Figures 6a and 6b, respectively) provide also important clues for the side chains of Glu (E) and Thr (T) residues: Of particular interest in the ATR FT-IR spectrum of the B_m1 peptide (Figure 6a) is a rather weak, but prominent and reproducible, band at 1722 cm^{-1} , which may be attributed to the C=O stretching vibration ($\nu(\text{C}=\text{O})$) of protonated carboxyl groups of the two Glu residues of the B_m1 peptide.²⁸ The spectral region $1710\text{--}1760 \text{ cm}^{-1}$ has the particular advantage that is generally free from overlap by other amino acid absorptions and it usually contains absorption bands originating from C=O stretching vibrations of protonated carboxyl groups of Glu (E) or Asp (D) residues.²⁸ The B_m1 peptide does not contain Asp (D) residues but only two Glu (E) residues (see Figure 1). There is no indication in the ATR FT-IR spectrum of the B_m1 peptide (Figure 6a) for the existence of a deprotonated carboxylate group, which usually shows a strong band near 1400 cm^{-1} ($\sim 1404 \text{ cm}^{-1}$) arising

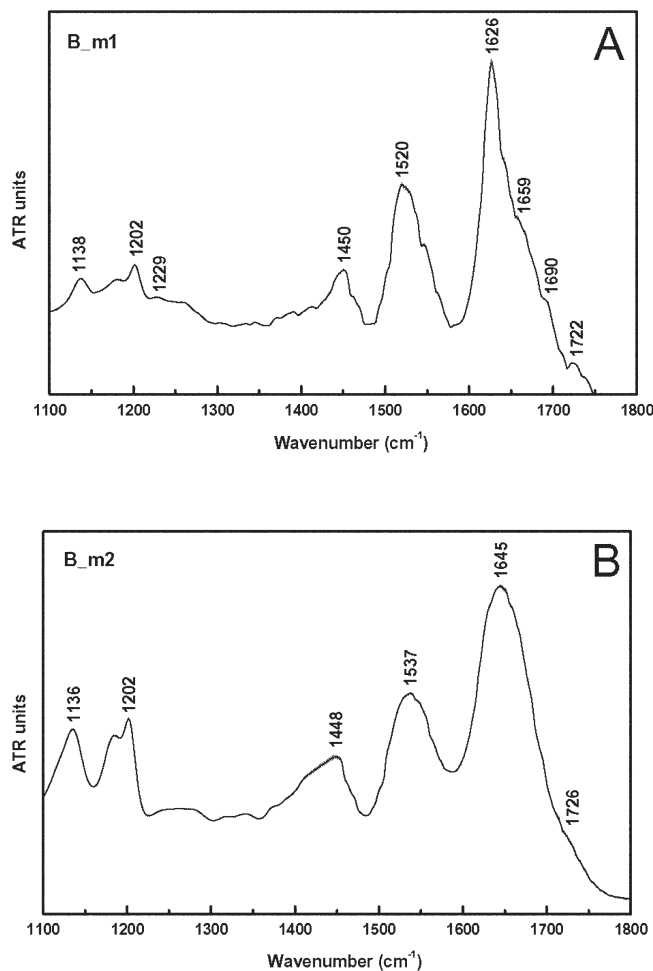


FIGURE 6 ATR FT-IR (900–1800 cm^{-1}) spectrum of B_m1 (A) peptide amyloid fibrils and B_m2 solution (B), cast on a Au mirror (see Materials and Methods). Errorbar equals 0.5σ in the IR spectrum.

from symmetric stretching of the COO^- ($\nu_s(\text{COO}^-)$) group.²⁸ It is perhaps interesting to mention, at this point, that in the ATR FT-IR and FT-Raman spectra of the B peptide, there is strong evidence, by strong bands at 1403 cm^{-1}

in both spectra, that the single Glu (E) residue of this peptide is deprotonated.⁷ In contrast, in the ATR FT-IR spectrum of the B_m2 peptide, there is no evidence other than a weak shoulder at 1726 cm^{-1} for the existence of protonated or deprotonated Glu (E) side chains, despite the fact that this peptide contains four⁴ Glu residues in its sequence (see Figure 1). In conclusion, it appears that the Glu (E) side chains of the B_m1 peptide, in the amyloid-like fibrils formed by this peptide, have C=O groups and COH groups, which may act both as hydrogen bond acceptors and donors, respectively.

Concerning the side chains of the three Thr (T) residues of the B_m1 and B_m2 peptides, there are strong bands at 1138 and 1136 cm^{-1} , respectively (Figures 6a and 6b), which may be attributed to C—O stretching vibrations of Thr side chains; strong bands in the spectral region 1075 – 1150 cm^{-1} are usually assigned to $\nu(\text{C—O})$ vibrations of Thr side chains,²⁸ whereas C—O stretching vibrations from Glu (E) side chains are usually located in the region 1120 – 1253 cm^{-1} . Thus, the rather strong bands at ca. 1200 cm^{-1} (there is a strong band at 1202 cm^{-1} and a weaker band at ca. 1180 cm^{-1} , in both B_m1 and B_m2 ATR FT-IR spectra, Figures 6a and 6b, respectively) may be due to $\nu(\text{C—O})$ vibrations from Glu (E) side chains.²⁸ Interestingly, a comparison of Figures 6a and 6b shows that all these bands are relatively stronger in the B_m2 peptide ATR FT-IR spectra.

Models Derived From the Data

Taking into account all experimental and theoretical evidence accumulated previously for silkmoth chorion proteins,⁵ as well as for synthetic peptide-analogues of parts of chorion proteins,^{6–7,13} the hexapeptide periodicities present in the central domain of the A and B families of chorion proteins (see also Figure 1) and the models presented by Iconomidou et al.,^{6,7} as plausible structures for the A and B families of chorion proteins, we propose the models shown in Figures 7a and 7b, as possible models for the structure of the B_m1

Table I Amide I, II, and III Infrared Wavenumber Ranges (cm^{-1}) and Their Dependence on Secondary Structure^{24–27} and Main ATR FT-IR Band Maxima (cm^{-1}) of B_m1 and B_m2 Peptides, as Determined From the Spectra

Band	Secondary Structure				B family peptide-analogues	
	α -helix	β -pleated sheet	β -turns	random/unordered	B_m1	B_m2
Amide I	1653–1660 or 1644–1649	1690–1699 and 1610–1640	1662–1695	1650–1654	1690 1659 1626	1645
Amide II	1548–1553 or 1519–1521	1543 or 1517–1535		1546–1553	1520	1537
Amide III	1280–1317	1230–1245		1245–1270	1229	

peptide by homology modeling to the structure of the cA peptide.⁶

The data presented here are clearly in favor of the antiparallel β -pleated sheet model shown in Figure 7a, but it should be mentioned that the left-handed parallel β -helix model of Figure 7b has attractive features as well. Most interesting among these is the hydrophobic core and hydrophobic faces of the triangular prism-like helix. Nevertheless, the “edges” of this prism are occupied by charged, polar residues and glycines and this makes 3D packing difficult, unless there are very specific interactions or the presence of water molecules among the packed β -helices. The hydrophobic faces of the antiparallel β -sheet structure shown in Figure 7a facilitate uniform 3D packing of the β -sheets, leaving the polar and charged residues on both lateral “edges” of the sheet for favorable lateral interactions.

Although we were the first, to our knowledge, to propose a detailed left handed parallel β -helix structural model, at atomic resolution, as a possible structure underlying amyloid fibrils,⁶ several groups after our proposal, suggested parallel β -helix models as models dictating formation of amyloid like fibrils.^{30–3533} Khurana and Fink³⁶ have tried to determine whether parallel β -helix proteins have a unique FT-IR spectrum, which would help in identifying parallel β -helices as structures underlying amyloid fibrils. However, they concluded that there is no unique infrared signature for parallel β -helix structure.

In summary, both ATR FT-IR spectroscopy and X-ray diffraction data for the B_m1 peptide, as well as evidence from the cA and B peptide data^{6,7} are in favor of the antiparallel β -sheet model of Figure 7a, which is a classical cross- β structure, compared to the left-handed parallel β -helix model of Figure 7b. Furthermore, evidence, mainly arising by calculating X-ray diffraction patterns of the models of Figures 7a and 7b, utilizing the software CLEARER,¹⁷ and comparing them with that obtained experimentally in Figure 5, presented in Figures 9a and 9b, is clearly in favor of the ladder, typical cross- β , model presented in Figure 7a. In this respect, it is very interesting to note that, very recently, Jahn et al.³⁷ have examined models that span from the classical cross- β through β -helices to native-like structures against experimentally obtained X-ray diffraction patterns, in a variety of amyloid cases, and they arrive at the same conclusion that the results support the long held belief in the classic cross- β model.²¹ Both models, the typical cross- β , presented in Figure 7a and the left handed parallel β -helix model presented in Figure 7b, cannot reproduce in the simulated diffractograms, a very sharp observed meridional reflection at 5.2 Å. The very sharp character of this meridional reflection implies a long range order, of a similar periodicity, in the oriented

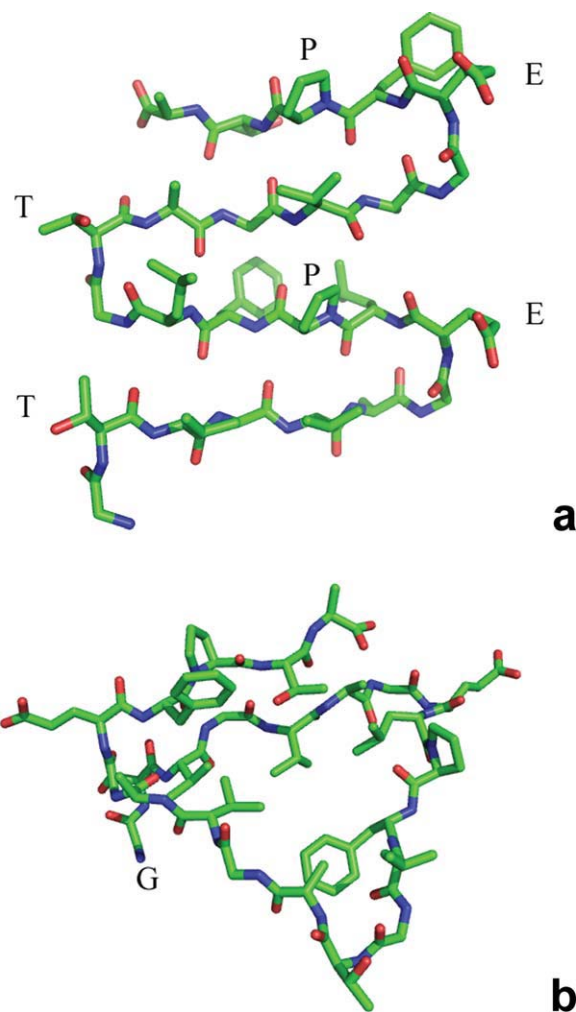


FIGURE 7 (a) Antiparallel twisted β -sheet model (“cross- β ” structure) proposed for the B_m1 peptide (stick representation utilizing the software PyMOL²⁹). Tentative type II’ β -turns alternate with four-residue β -strands.⁶ View almost perpendicular to the “face” of the β -sheet. Glutamate (E) and Threonine (T) residues, located at the β -turns, in the opposite “edges” of the β -sheet, and Proline (P) residues located in the β -strands are seen. (b) Stick representation of the B_m1 peptide in a left-handed parallel β -helix conformation (ca. one and a half turn of the helix). Tentative type II β -turns alternate with β -strands. View at an angle to the axis of the helix. The first residue of the peptide (a Glycine, G) is shown. The software PyMOL²⁹ was used.

fibers formed from the amyloid fibrils of the B_m1 peptide, along the fiber axis, which should coincide with the direction of the hydrogen bonds formed between successive β -strands. The value of 5.2 Å is reminiscent of the periodicity arising from the pitch of α -helices in a coiled-coil conformation. However, neither experimental nor theoretical evidence (secondary structure prediction, data not shown) supports the existence of α -helices in the structure of the B peptides. Another plausible possibility might be a periodicity arising

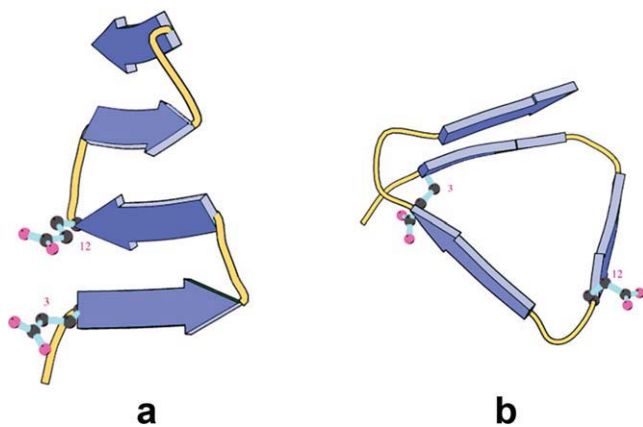


FIGURE 8 (a) A schematic antiparallel twisted β -sheet model (“cross- β ” structure) for the B_m2 peptide (ribbon representation utilizing the software MOLSCRIPT³⁸), with the side-chains of the two glutamate (E) residues that have replaced one valine (V) and one leucine (L) residues, of the B_m1 peptide (cf. Figure 1) as ball and sticks. Arrows represent β -strands. Tentative type II’ β -turns alternate with four-residue β -strands.⁶ View almost perpendicular to the “face” of the β -sheet. It is clear that this structure is not favorable because of strong repulsive electrostatic interactions of the glutamate side chains in close proximity. (b) A ribbon representation of the B_m2 peptide in a left-handed parallel β -helix conformation with the side-chains of the glutamates (as in (a) above) added as balls and sticks. Tentative type II β -turns alternate with β -strands. Arrows represent β -strands. View parallel to the axis of the helix. It is evident that this structure is not favorable because the side chains of, at least, one glutamate residue is buried into the hydrophobic interior of the left-handed parallel β -helix.

from periodical structural features derived from the amino acid sequence itself. In that respect, it is interesting to note that the average distance of the side chains of two glutamates (E) and two threonines (T), on the turns, is ca. 10.4 Å, in the ladder model for B_m1 (Figure 7a), twice that of the periodicity corresponding to the observed sharp reflection at 5.2 Å.

In contrast, for peptide B_m2, none of these models seem to be a favorable structure as shown in Figures 8a and 8b. In the ladder model (Figure 8a) glutamates are very close to each other, which results to unfavorable electrostatic interactions, and, in the left-handed helix model (Figure 8b), a glutamate, at least, is located into the hydrophobic interior of the β -helix, which results to a very unstable structure. Therefore, it appears that none of the models is a favorable one in the case of the B_m2 peptide, which easily explains the fact that this peptide does not form amyloid fibrils even after incubation for several months.

A rather very important finding of this work, also supported by our previous findings,⁷ is that peptide-analogues of parts of the B family central domain, tend to aggregate laterally and in register (Figures 2b and 2c), forming ribbons of parallel fibrils, which may extend under presumably favorable conditions, to form planar extended surfaces of parallel and in register fibrils, a process that apparently mimics in many respects the self-assembly process *in vivo*, where planes of fibrils self-assemble to form silkmoth cho-

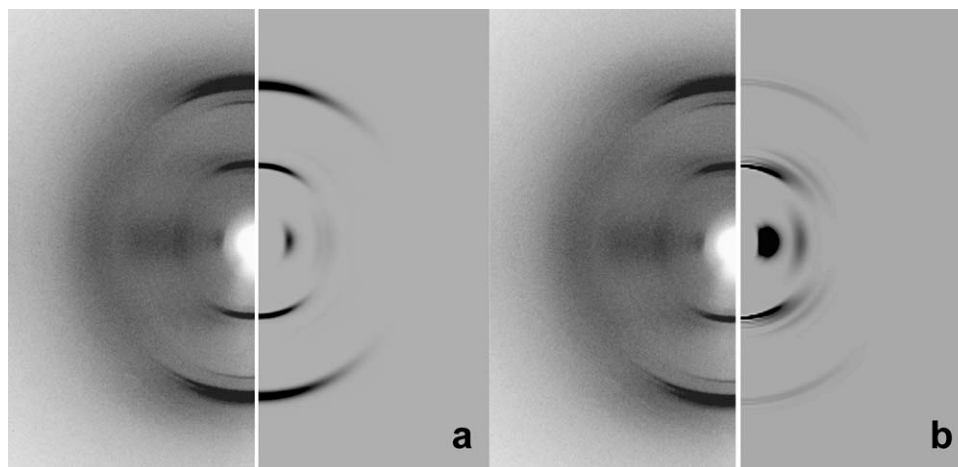


FIGURE 9 (a) A comparison of the experimentally observed X-ray diffraction pattern from an oriented fiber of B_m1 peptide amyloid-like fibrils (left half, Figure 5), with that calculated (right half), utilizing the software CLEARER,¹⁶ from the typical cross- β model (ladder model) of the B_m1 peptide, shown in Figure 7a. Details are given in “Materials and Methods”. (b) A comparison of the experimentally observed X-ray diffraction pattern from an oriented fiber of B_m1 peptide amyloid-like fibrils (left half, Figure 5), with that calculated (right half), utilizing the software CLEARER,¹⁷ from the left-handed parallel β -helix model of the B_m1 peptide, shown in Figure 7b. Details are also given in “Materials and Methods”. It is clearly seen that the simulation indicates as most favorable model that of the typical cross- β structure of Figure 7a.

rion lamellae. These lamellae consist of planes of fibrils twisted in a helicoidal manner.^{5,39,40} The *in vitro* self-assembly process leads to the formation of gels (data not shown), with, at present, unknown properties. Further, more detailed and refined work is perhaps needed to explore the properties and possible future applications of the so-formed gels. The lateral interactions between fibrils may be dictated by precise, favorable hydrogen bonds between the side chains of two threonines (T) and two glutamates (E) occupying the opposite “edges” of the antiparallel β -pleated sheets (Figure 7a) of the B_{m1} peptide. However, despite the rich spectroscopic evidence presented above, it is difficult to delineate in detail the exact network of such hydrogen bonds, because the side chains of both residues have the ability to act both as hydrogen bond donors or acceptors.

In conclusion, we have shown in this work that: (a) a peptide with a length ca. half of the central conservative domain of the B family silkworm chorion proteins and six residues longer than the previously studied B peptide,⁷ folds and self-assembles into amyloid fibrils almost identical in properties with those of the B peptide (which corresponds to a smaller part of the entire length of the B family central domain), and this is in strong support of our previous proposal that silkworm chorion is a natural protective amyloid^{6,23} and, (b) that by performing carefully designed mutations of β -sheet ‘former’ residues on the sequence of these amyloidogenic peptides, we managed to easily prevent the formation of amyloid structure. Similarly designed mutations in other cases of destructive amyloidoses, coupled with our recent finding that amyloidogenic determinants lie mainly on the surface of native proteins causing amyloidoses, instead of being buried into the hydrophobic cores of these proteins,⁴¹ may provide useful clues for future studies aiming at a remedy of the serious diseases caused by amyloid formation.

The authors thank the reviewers of this manuscript for their useful and constructive criticism.

REFERENCES

- Kafatos, F. C.; Regier, J. C.; Mazur, G. D.; Nadel, M. R.; Blau, H. M.; Petri, W. H.; Wyman, A. R.; Gelinas, R. E.; Moore, P. B.; Paul, M.; Efstratiadis, A.; Vournakis, J. N.; Goldsmith, M. R.; Hunsley, J. R.; Baker, B.; Nardi, J.; Koehler, M. The eggshell of insects: Differentiation-specific proteins and the control of their synthesis and accumulation during development; Springer-Verlag: Berlin, Heidelberg, New York, 1977.
- Regier, J. C.; Kafatos, F. C. Molecular aspects of chorion formation; Pergamon Press: Oxford, New York, 1985.
- Hamodrakas, S. J.; Jones, C. W.; Kafatos, F. C. *Biochim Biophys Acta* 1982, 700, 42–51.
- Lekanidou, R.; Rodakis, G. C.; Eickbush, T. H.; Kafatos, F. C. *Proc Natl Acad Sci USA* 1986, 83, 6514–6518.
- Hamodrakas, S. J. Molecular architecture of helicoidal proteinaceous eggshells; Springer-Verlag: Berlin and Heidelberg, 1992; Chapter 6.
- Iconomidou, V. A.; Vriend, G.; Hamodrakas, S. J. *FEBS Lett* 2000, 479, 141–145.
- Iconomidou, V. A.; Chryssikos, G. D.; Gionis, V.; Vriend, G.; Hoenger, A.; Hamodrakas, S. J. *FEBS Lett* 2001, 499, 268–273.
- Iconomidou, V. A.; Hamodrakas, S. J. *Current Protein Pept Sci* 2008, 9, 291–309.
- Pepys, M. B. *Amyloidosis*; Oxford University Press: Oxford, UK, 1996.
- Kelly, J. W. *Curr Opin Struct Biol* 1996, 6, 11–17.
- Kelly, J. W. *Curr Opin Struct Biol* 1998, 8, 101–106.
- Dobson, C. M. *Trends Biochem Sci* 1999, 24, 329–332.
- Iconomidou, V. A.; Chryssikos, G. D.; Gionis, V.; Galanis, A. S.; Cordopatis, P.; Hoenger, A.; Hamodrakas, S. J. *J Struct Biol* 2006, 156, 480–488.
- Collaborative Computational Project, Number 4 *Acta Cryst* 1994, D50, 760–763.
- De Jongh, H. H. J.; Goormaghtigh, E.; Ruyschaert, J. M. *Anal Chem* 1996, 242, 95–103.
- Savitsky, A.; Golay, M. J. E. *Anal Chem* 1964, 36, 1627–1639.
- Makin, O. S.; Sikorski, P.; Serpell, L. C. *J Appl Cryst* 2007, 40, 966–972.
- Sikorski, P.; Atkins, E. D. T.; Serpell, L. C. *Structure* 2003, 11, 915–926.
- Fraser, R. D. B.; McRae, T. P. *Conformation in fibrous proteins and related synthetic polypeptides*; Academic Press: New York, 1973.
- Keith, H. D.; Giannoni, G.; Padden, F. J. *Biopolymers* 1969, 7, 775–792.
- Geddes, A. J.; Parker, K. D.; Atkins, E. D. T.; Beighton, E. J. *Mol Biol* 1968, 32, 343–358.
- Krejchi, M. T.; Cooper, S. J.; Deguchi, Y.; Atkins, E. D. T.; Fournier, M. J.; Mason, T. L.; Tirrell, D. A. *Macromolecules* 1997, 17, 5012–5024.
- Hamodrakas, S. J.; Hoenger, A.; Iconomidou, V. A. *J Struct Biol* 2004, 145, 226–235.
- Krimm, S.; Bandekar, J. *Adv Prot Chem* 1986, 38, 181–386.
- Surewicz, W.K.; Mantsch, H.H.; Chapman, D. *Biochemistry* 1993, 32, 389–394.
- Haris, P. I.; Chapman, D. *Biopolymers (Pept Sci)* 1995, 37, 251–263.
- Parker, F. S. *Applications of infrared spectroscopy in biochemistry, biology and medicine*; Plenum Press: New York, 1971.
- Barth, A. *Prog Biophys Mol Biol* 2000, 74, 141–173.
- Delano, W. L. 2005. The PyMOL molecular graphics system. In DeLano Scientific LLC 400, Oyster Point Blvd., Suite 213, South San Francisco, CA 94080-1918.
- Wille, H.; Mitchelitsch, M. D.; Guénebaut, V.; Supattapone, S.; Serban, A.; Cohen, F. E.; Agard, D. A.; Prusiner, S. B. *Proc Natl Acad Sci* 2002, 99, 3563–3568.

31. Wetzel, R. *Structure* 2002, 10, 1031–1036.
32. Pickersgill, R. W. *Structure* 2003, 11, 137–138.
33. Williams, A. D.; Portelius, E.; Kheterpal, I.; Guo Jun-Tao; Cook, K. D.; Hu, Y.; Wetzel, R. *J Mol Biol* 2004, 335, 833–842.
34. Kishimoto, A.; Hasegawa, K.; Suzuki, H.; Taguchi, H.; Namba, K.; Yoshida, M. *Biochem Biophys Res Comm* 2004, 315, 739–745.
35. Govaerts, C.; Wille, H.; Prusiner, S. B.; Cohen, F. E. *Proc Natl Acad Sci USA* 2004, 101, 8342–8347.
36. Khurana, R.; Fink, A. L. *Biophys J* 2000, 78, 994–1000.
37. Jahn, T. R.; Makin, O. S.; Morris, K. L.; Marshall, K. E.; Tian, P.; Sikorski, P.; Serpell, L. C. *J Mol Biol* 2010, 395, 717–727.
38. Kraulis, P. J. *J Appl Crystallogr* 1991, 24, 946–950.
39. Bouligand, Y. *Tissue and Cell* 1972, 4, 189–217.
40. Neville, A. C. *Phys Bull* 1986, 37, 74–76.
41. Frousios, K. K.; Iconomidou, V. A.; Karletidi, C.-M.; Hamodrakas, S. J. *BMC Struct Biol* 2009, 9, 44.